universität wien

MASTERARBEIT / MASTER'S THESIS

Titel der Masterarbeit / Title of the Master's Thesis

„Lipophilicity, Binding Affinity and Toxicity of Potential Ligands for Muscarinic Acetylcholine Receptors“

verfasst von / submitted by

Julia Seunig, BSc

angestrebter akademischer Grad / in partial fulfilment of the requirements for the degree of

Magistra pharmaciae (Mag.pharm.)

Wien, 2023 / Vienna 2023

Studienkennzahl lt. Studienblatt / degree programme code as it appears on the student record sheet:	UA 066 605
Studienrichtung lt. Studienblatt / degree programme as it appears on the student record sheet:	Masterstudium Pharmazie
Betreut von / Supervisor:	Ass.-Prof. Mag. Dr. Verena Pichler

Acknowledgement

First of all, I would like to thank my supervisor Ass.-Prof. Mag. Dr. Verena Pichler, who always supported me with words and deeds and invested so much patience and time in the supervision of my master thesis.

I would also like to thank Marius Ozenil, PhD who not only explained all the work processes and equipment to me, but also helped me with any questions and uncertainties with an incredible calmness and composure.

I would also like to thank Marlon Millard, MSc for synthesizing the test compounds and the entire Nuclear Medicine team.

Most of all, I would like to thank my father, who always supported me and believed in me, even when I often could not do it myself. Thanks to my grandparents, who were always there for me in every situation. I would also like to thank my mother for her support, especially in the last year. Without you all this would not have been possible.

Abstract

Muscarinic acetylcholine receptors (mAChRs) belong to the G-protein-coupled receptors and are divided into five subtypes. They play a critical role in both the central and peripheral nervous systems. Due to the fact, that they regulate many neuronal functions, they are often associated with neurological diseases, such as Alzheimer's or Parkinson's disease. The localization and the different function of the subtypes vary considerably, so that the development of subtype-selective ligands, which can be applied as PET tracers, is of great interest for pharmaceutical research. The aim of this master thesis is to identify potential ligands that have a strong affinity for the mAChRs and ideally also a good subtype selectivity. The ligands to be investigated are structurally related to the recently identified rearrangement product of the M1 receptor antagonist Pirenzepine. First, the compounds were analyzed for purity and their lipophilicity (logP) by means of HPLC. An MTT assay was performed to assess an potential effect on cell proliferation of the analytes. The affinity of the 22 ligands under investigation was evaluated using a competitive radioligand binding assay. The most promising compounds (Mima187, Mima194), which showed effective displacement toward the Tritium-labelled N-Methyl-scopolamine in a fast screening procedure, were tested for their K_i values using the Cheng-Prusoff equation.

Kurzfassung

Die muskarinischen Acetylcholinrezeptoren (mAChRs) gehören zu den G-Protein-gekoppelten Rezeptoren und sind in fünf Subtypen unterteilt. Sie spielen eine entscheidende Rolle sowohl im zentralen als auch im peripheren Nervensystem. Aufgrund der Tatsache, dass diese Rezeptoren viele neuronale Funktionen regulieren, werden sie oft mit neurologischen Erkrankungen, wie Alzheimer oder Parkinson in Verbindung gebracht. Die Lokalisation und die unterschiedliche Funktion der Subtypen variieren sehr stark, sodass die Entwicklung von subtypselektiven Liganden, welche als PET Tracer Anwendung finden könnten, ins Interesse der pharmazeutischen Forschung rückt. Das Ziel dieser Masterarbeit besteht darin potenzielle Liganden zu identifizieren, welche eine starke Affinität zu den mAChRs aufweisen und optimalerweise eine gute Subtypselektivität besitzen. Bei den zu untersuchenden Liganden handelt es sich hierbei um strukturelle verwandte Verbindung angelehnt an ein kürzlich gefundenes Umlagerungsprodukt des M1-Rezeptorantagonsiten Pirenzepin. Zunächst wurden die Verbindungen auf ihre Reinheit untersucht und anschließend deren Lipophilie (logP) mit Hilfe von einer HPLC analysiert. Die Verbindungen wurden auch auf ihre Toxizität in einem MTT Test untersucht. Die Bewertung der Affinität der 22 Liganden zu den mAChRs erfolgte mit Hilfe eines kompetitiven Radioliganden-Bindungstests. Die vielversprechendsten Verbindungen (Mima187, Mima194), welche eine effektive Verdrängung gegenüber dem Tritium markierten N-Methyl-scopolamin in einem Schnelldetektionverfahren aufwiesen, wurden weitergetestet um die K_i-Werte mit Hilfe der Cheng-Prusoff-Gleichung zu bestimmen.

Contents

Introduction

Dementia and Alzheimer disease

Dementia diseases represent an enormous burden both for those affected and for caregivers. Due to the progressive impairment of brain performance, dementia patients experience enormous physical and emotional changes, which become noticeable primarily through memory loss, communication, and speech disorders, as well as the loss of logical thinking in the environment. Alzheimer's disease (AD) is the reason for the onset of dementia in around 60 to 80 percent of cases.[1]

AD, which is associated with progressive memory loss and dementia, is the one of the most common neurodegenerative diseases. The disease is characterized by the presence of extracellular deposits of amyloid-β-peptide in the form of fibril aggregates forming senile plaques and degeneration of presynaptic cholinergic neurons.[2]–[4]

Figure1 shows a positron emission tomography scan of the brain of a healthy person compared to an Alzheimer`s patient.[5]

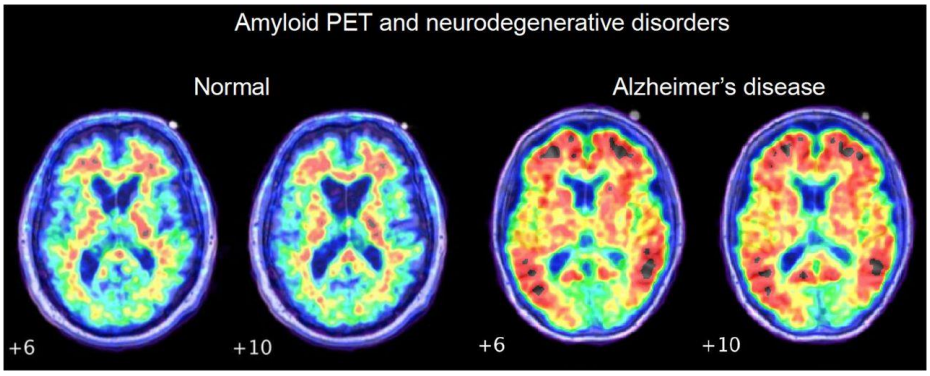

Figure1: Positive [^{11}C]PIB scan: normal vs. Alzheimer's disease.[5]

Dementia and Parkinson disease

Dementia is also of enormous clinical importance in Parkinson's disease (PD). It is estimated that 10 percent of Parkinson's patients suffer from dementia each year.[6]

In PD, there is an imbalance between striatal Dopamine and Acetylcholine.

The antidyskinetic effect of the anticholinergics used is based on restoring the balance, which in the case of PD is shifted toward cholinergic activity. The problem with those

agents is the occurrence of peripheral and central side effects, in particular urinary retention, nausea and constipation, as well as cognitive impairment.[7], [8]

In the clinic, L-DOPA is primarily used to treat the disease. Anticholinergics play a minor role here primarily due to the range of side effects. However, non-selective antagonists are the only muscarinic acetylcholine receptors (mAChRs) ligands currently used for the treatment of PD. Thus, the main focus of mAChR drug discovery for PD is to discover selective antagonists with the hope of minimizing side effects and achieving a better quality of life for Parkinson's patients.[9], [10]

Muscarinic acetylcholine receptors and their clinical application

mAChRs belong to the G-protein-coupled receptors. They are categorized into five subtypes (M1, M2, M3, M4, M5). Those receptors differ in their expression pattern and downstream signal transduction.[11]

In terms of their signal transduction, they can be divided into two distinct groups. M1, M3 and M5 mAChR subtypes couple via $G_{q/11}$ proteins. They activate phospholipase-C and mobilize intracellular calcium, as shown in figure2.

M2 and M4 mAChRs, on the other hand, belong to the group of $G_{i/o}$ -protein-coupled receptors and inhibit adenylate cyclase (AC), leading to an overall reduction in the intracellular concentration of cAMP (cyclic Adenosine Monophosphate) (see table1).[9]

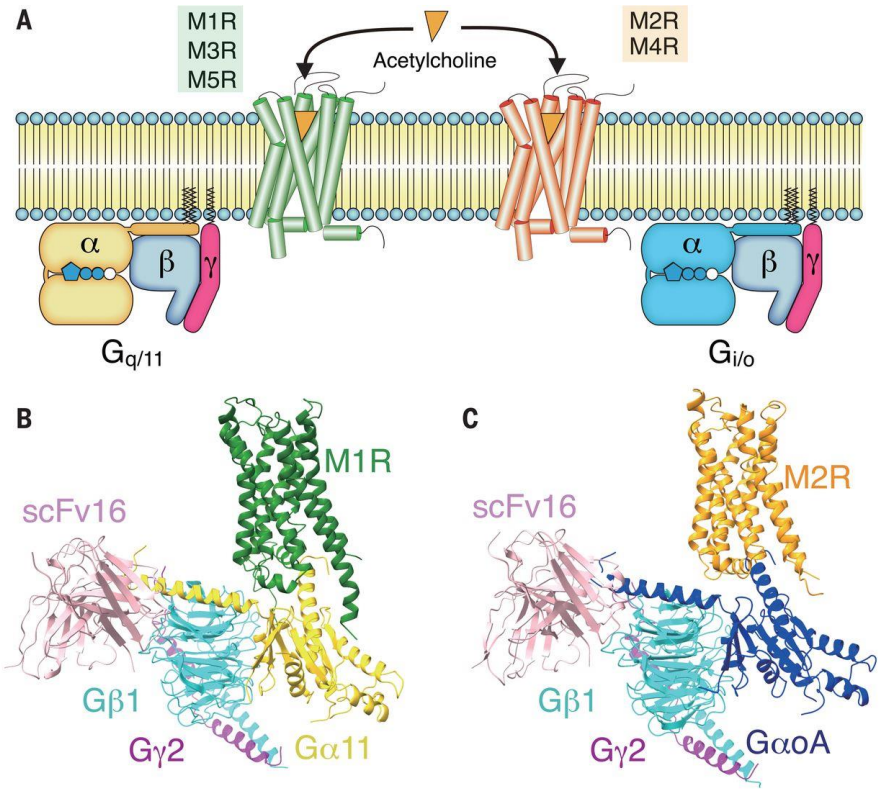

Figure2: (A) Signal transmission of the mAChRs (B) cryo-electron microscopy structure of a M1 mAChR, (C) cryo-electron microscopy structure of a M2 mAChR.[12]

The different expression patterns of the subtype variations make the mAChRs interesting targets for the therapy of many diseases affecting the central nervous system (CNS), such as AD and PD, as well as for those diseases originating in the body periphery. The following table1 shows examples of classification, ligand selectivity, tissue distribution and function of mAChRs.[9]

Table1: Examples of agonists, antagonists for mAChR subtypes where they are localized and its function.[13]

mAChR-subtype	M1	M2	M3	M4	M5
Agonist	Muscarine, Pilocarpine	Muscarine, Pilocarpine	Muscarine, Pilocarpine	Muscarine, Pilocarpine	Muscarine, Pilocarpine
Antagonist	Pirenzepine, Atropine	Atropine, Scopolamine	Darifenacine, Solifenacine	Atropine, Scopolamine	Atropine, Scopolamine
Tissue	Central-and peripheral nervous system	Heart, central nervous system	Gastrointestinal tract, urinary tract, central nervous system	Central nervous system	Central nervous system
Function	Neuronal excitation, memory	Frequency- and contractility de-crease, memory	Frequency- and contractility de-crease, memory	Analgesia	Memory

Muscarinic receptors are present in both the body periphery and the central nervous system. Muscarinic receptor agonists mimic the action of the parasympathetic nervous system in the body periphery and are therefore also called parasympathomimetics. Important representatives of that group are: Acetylcholine, Bethanechol, Carbachol Arecoline and Pilocarpine. Structures are illustrated in figure3. With the exception of Pilocarpine and Arecoline, these substances are quaternary ammonium compounds at a physiological pH. Important structural features of the substances are the quaternary nitrogen (Acetylcholine, Bethanechol, Carbachol) or the protonable nitrogen (Arecoline, Pilocarpine) and the ester or ether oxygen in each structural formula. Due to their pharmacological structural features, these representatives show low absorption from the gastrointestinal tract. In therapeutic practice, mainly Pilocarpine and Carbachol are used in the form of eye drops.[14]

mAChR agonists are generating interest as potential therapeutics for the treatment of AD. However, none of the compounds tested have reached phase IV.[15] Reasons for this were on the one hand the lack of selectivity for the M1 mAChR on the other hand a too low safety margin as well as bioavailability and poor tolerability.[16]–[18]

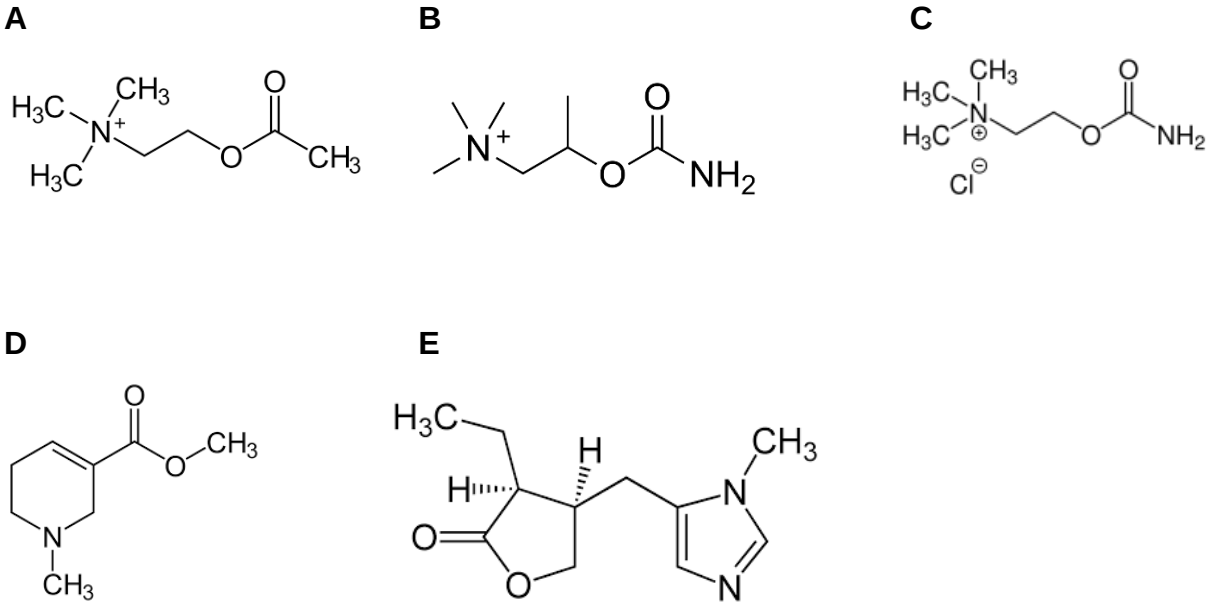

Figure3: Structures of: (A) Acetylcholine, (B) Bethanechol, (C) Carbachol, (D) Arecoline, (E) Pilocarpine.

Muscarinic receptor antagonists inhibit the action of the parasympathetic nervous system and are therefore also called parasympatholytics. Representatives of this group play a central role in the treatment of PD. The lead substance of these antagonists is Atropine. The natural alkaloids Atropine and Scopolamine are the main constituents of Belladonna. Chemically, they are esters of tropic acid.

Other representatives of the group are: Ipratropium, Butylscopolamine, Oxybutynin, Pirenzepine, Tropicamide, and Metixene and Biperidene. Those structures are shown in figure4.The first two active ingredients, Oxybutynin and Butylscopolamine, are quaternary amines and, due to their polarity, can hardly penetrate the blood-brain barrier. In practice, they are used as spasmolytics. The equally polar Ipratropium is used in asthma therapy in the form of inhalers. The latter two substances, Biperiden and Metixen, are used in the treatment of PD. Their therapeutic effect is based on the blockade of the excessively activated strial muscarinic receptors.

Both substances are overall better able to cross the blood-brain barrier than the other Atropine-like substances because they are not quaternary ammonium compounds. The main use of Pirenzepine is in ulcer therapy. This muscarinic receptor antagonist is characterized by a high degree of suptype specificity. Pirenzepine has a 100-fold higher affinity for M1 receptors than for the other subtypes. The selective M1 antagonist is central to this work due to its structural properties.[14]

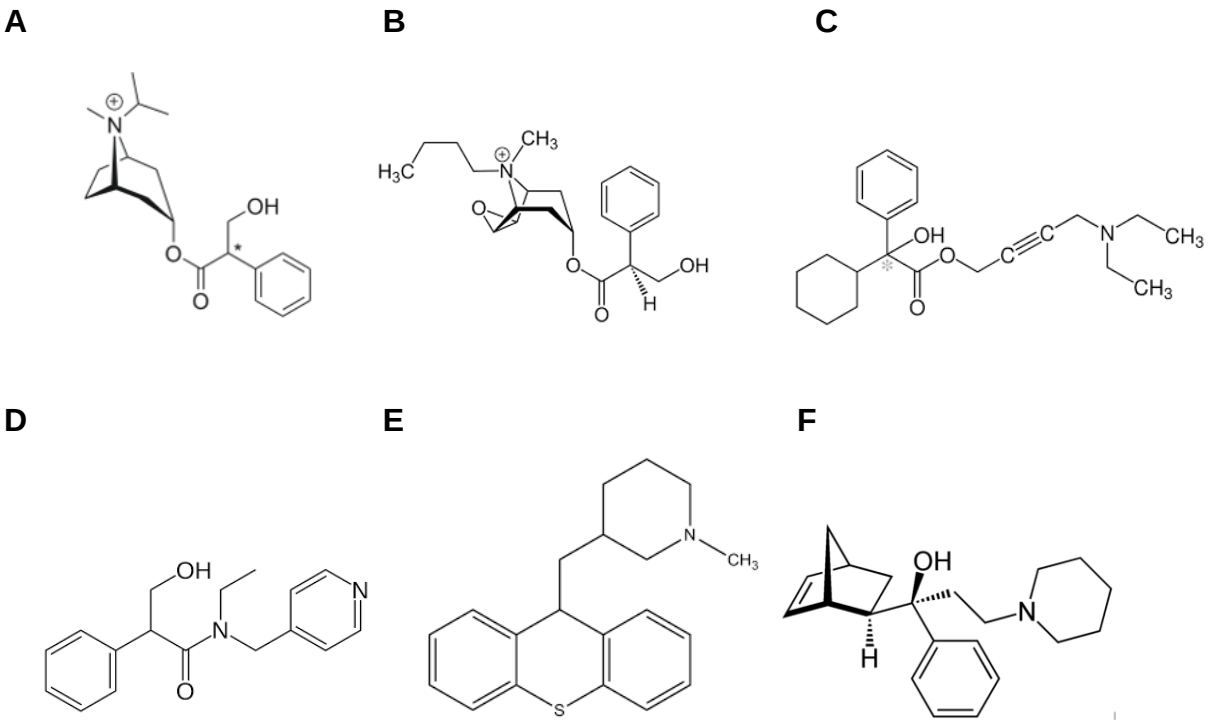

Figure4: Structures of: (A) Ipratropium, (B) Butylscopolamin, (C) Oxybutinin, (D) Tropicamide, (E) Metexine, (F) Biperidin.

This work essentially aims to identify ligands as potential therapeutics for neurodegenerative diseases. The following table2 illustrates the localization of the subtypes in the different brain areas and shows the associated relevance for the disease.

Table2: Expression profile of mAChRs and disease relevance of the different mAChR subtypes.[9]

mACh subtype	**M1**	**M2**	**M3**	**M4**	**M5**
Preferred signal trans-duction	Gq/11 PLC IP_3/DAG Ca^{2+}/PKC	Gi/o AC	Gq/11 PLC IP_3/DAG Ca^{2+}/PKC	Gi/o AC	Gq/11 PLC IP_3/DAG Ca^{2+}/PKC
Expression profile	Cerebral cortex, hippocampus striatum, thalamus	Hindbrain, thalamus, Cerebral cortex, hippocampus striatum, smooth muscle, heart, lung	Cerebral cortex, hippocampuss mooth muscle, glandular tissues	Striatum, cerebral cortex, hippocamps	Substantia nigra
Disease relevance	Alzheimer`s disease, Cognitive dysfunction	Alzheimer`s disease, Cognitive dysfunction, pain	Chronic obstructive pulmonary disorder, urinary incontinence	Parkinson`s disease, neuropathic pain	Drug dependence Parkinson´s disease

M1 subtype is localized in cortex, hippocampus, striatum and thalamus. Especially cortex as well as hippocampus are among those areas that play a central role in learning and memory. It represents a potential key therapeutic target for the treatment of AD.[19]

M2 mAChRs are localized in the brain, where they are mainly found in the cortex, hippocampus, striatum and thalamus. Furthermore, they are expressed in the heart and are thus also considered as potential targets for the development of new drugs targeting cardiovascular control.[20], [21]

M3 mAChRs are expressed in the brain, where they are mainly located in the cortex and hippocampus. They are also localized in smooth muscle and glandular tissue, which explains their role in triggering contraction.[22],[23]
M4 mAChRs are found in the cortex as well as the hippocampus, but also in the striatum, where they are thought to play a role in controlling dopamine release.[24]
M5 mAChRs show discrete localization in the substantia nigra. It is found primarily in midbrain dopaminergic neurons. For this reason, it is a potential target for therapy of PD as well as drug addiction.[25]

Drug development process

The development of new drugs is a very lengthy, complex and expensive process. The time to bring a new drug to market averages 10 years and often costs over a billion dollars. The following figure5 illustrates the phases of drug development including basic research and discovery, as well as preclinical research through to clinical development and the post-marketing period.[26] [27]

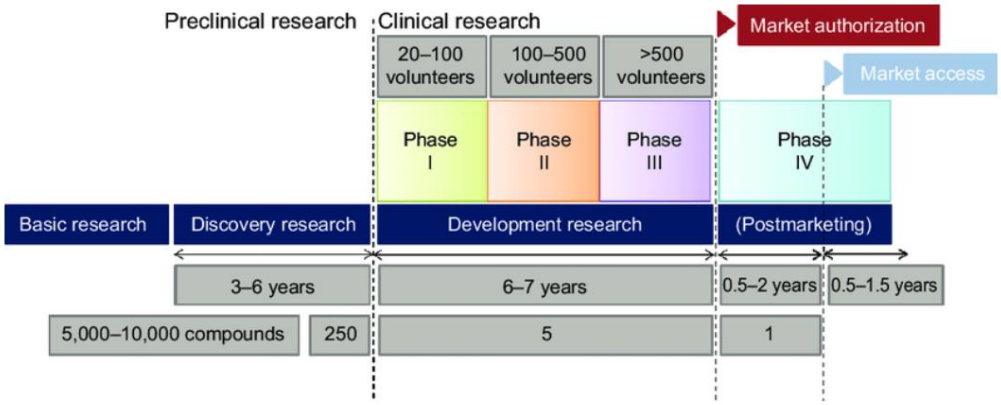

Figure5: Schematic representation of the drug development process.[27]

The process generally starts with an idea, which often results from minute observations or everyday routine activities in the laboratory. As can be seen from the figure5, important points of preclinical drug development are basic research and discovery research, where the main focus is on a suitable selection of test substances and their characterization. In the preclinical phase, no human trials are performed yet.

Only after a large number of in vitro experiments and animal studies, in which the effect and tolerability have been characterized in a preliminary overview, does clinical testing in humans take place. This clinical development period is divided into four phases. In Phase I, the aim is to gain knowledge about tolerability, distribution, absorption, biotransformation and elimination. This Phase I study is conducted with healthy volunteers. Phase II studies focus on testing the efficacy of the drug in a specific indication and dose finding. The subsequent Phase III study aims to gather evidence of therapeutic benefit. Here, a large patient population (>500 subjects) is used, ideally to conduct randomized double-blind studies. Within the Phase IV studies, the drug is already administered in the approved indication, dosage and duration of use and potential interactions can thus be uncovered.[14]
This work focuses exclusively on preclinical phase issues in drug development, including primary assays, affinity measurements, and cell viability assays.

Positron Emission Tomography

The pharmaceutical industry has paid particular attention to functional imaging over the past decade. Promising prospects for the diagnosis of AD and PD are offered in particular by PET (positron emission tomography) radiotracers targeting mAChRs. In this context, new therapeutic options for dementia could develop.[28]
PET tracers are mainly used in oncological or cardiac imaging on the one hand to assess the stages and analyse the progression of the disease and on the other hand to monitor the therapy.[29], [30]

The principle of PET imaging is based on the emission of a positron by a neutron-poor radioisotope. As soon as the radioisotope decays, the emitted positron travels a short distance of about 1-2 mm and encounters an electron. Electron and positron annihilate and two high energy photons result. The photons, moving linearly in opposite directions, can be detected outside the body with the PET scanner (See figure6).[31]

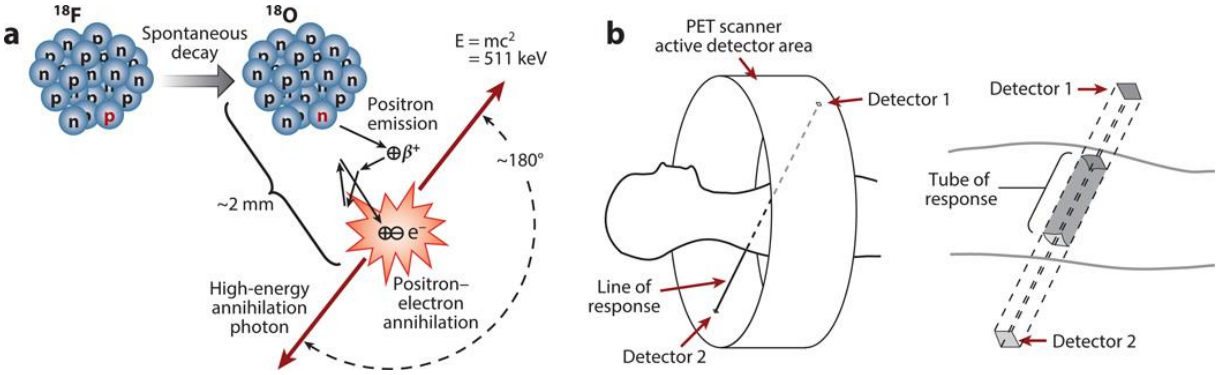

Figure6: (a) 511 keV annihilation photons produced by radioactive decay of Fluorine-18 (18F) (half-life 110 min) after positron emission has occurred. (b) Schematic representation of the positron emission tomography (PET) imaging process.[31]

In particular, small molecules of PET tracers for brain imaging have been developed in the last decades. The most common small molecule radiotracers include: 2-[^{18}F]FDG (2-[^{18}F]Fluoro-2- deoxy-D-glucose), [^{11}C]PIB (Pittsburgh compound B), [^{11}C]Raclopride, [^{11}C]Methionine, and [^{11}C]DASB (3-amino-4-(2-dimethylaminomethylphenylsulfanyl)-Benzonitrile). Of note here is the PET tracer [^{11}C]PIB which is specifically used particularly for imaging cerebral β-amyloid plaques and thus has applications in studies of neurodegenerative diseases.[28], [32]

Pirenzepine and its rearrangement products applied for structure identification

Pirenzepine itself is a representative of parasympatolytics. Those agents lead to the abolition of the parasympathetic effect by blocking the mAChR.[14]
Pirenzepine itself is considered an antagonist for mAChRs and has a high affinity for the M1 mAChR. Due to its inability to cross the blood-brain barrier, only peripheral mAChRs are affected by antagonism. In practice, Pirenzepine is used to treat gastric and duodenal ulcers by inhibiting gastric acid secretion and gastric motility.[33], [34]

The discovery and development of suitable ligands is often based on a trial-and-error approach. The discovery of the structure of the rearrangement product happened by chance in the course of a quality check. The structures of both Pirenzepine and its rearrangement product have identical molecular masses.

The rearranged products of Pirenzepine show significantly lower affinity toward all mAChR subtypes. Structural modifications were made to achieve higher affinity.
Both the Pirenzepine and its rearrangement product (figure7) have a Benzimidazole in their basic structure. For the introduction of a radiolabel in the form of a carbon-11 by a nucleophilic substitution reaction, the Methylpiperazine represents the ideal entry site for the radiolabel.[35]

A **B**

Figure7: (A) Structure of Pirenzepine, (B) rearrangement product of Pirenzepine.

Drug parameters for radiotracers

Several potential PET tracers for brain imaging have been discovered in the last decades. Overall, an ideal PET tracer targeting the human brain should meet several important design and testing criteria.

Important design criteria include selection of an appropriate target, high affinity and selectivity for the target, simplification of radiosynthesis, and maximization of target accessibility while minimizing nondisplaceable binding.

In addition, it is critical that some testing criteria be met, such as a good signal-to-noise ratio in vivo, low levels of radiolabelled metabolites in the target region, high sensitivity to the target, and that the in vivo distribution and pharmacology be consistent with literature reports.

Design criteria play a role with respect to the identification of appropriate candidates for PET tracer development while test criteria summarize properties to determine potential utility as radiotracers.[36]

In addition to these criteria, the blood-brain barrier plays a central role for those PET tracers that are used in the brain. Thus, the ideal PET tracer for the brain must be able to cross the blood-brain barrier using active transporters or passive diffusion. Active transporters are required to meet the brain's demand for important molecules such as amino acids and Glucose. These transporters can be used as entry points for tracers. However, most tracers do not have the structural properties to act as substrates for these transporters. Therefore, they rely largely on passive diffusion.[37]

Lipinskis rule of five

Christopher A. Lipinski observed that most oral drugs are relatively small and low-lipophilic molecules. Based on this finding, he first formulated the rule of Five in 1997. Lipinskis rule of five is still a fundamental reference point in pharmaceutical research for estimating the oral bioavailability of newly developed drugs. Although the rule of five is mostly applied to oral drugs in the literature, it can be assumed that it also applies to drugs that are intended to cross the blood-brain barrier. The focus is on the pharmacokinetic properties of the drug, including aspects related to its absorption, distribution, metabolism and excretion (ADME).[35]

Lipinski focused on four main parameters: Molecular weight, logP, number of H-bond donors and number of H-bond acceptors. Here, limits were set for each of the four parameters, which were all close to 5 or a multiple of five. This gave rise to the name "rule of 5".

For good permeation or absorption, it is considered crucial that the following criteria are met: the molecular weight should be less than 500, logP value less than 5, fewer than 5 H-bond donors (expressed as the sum of OHs and NHs) and the sum of H-bond acceptors (expressed as the sum of Ns and Os) should be less than 10.

Over the years, the rules have been further developed. The focus here has been to improve the prediction of drug-friendliness.[38]

Preclinical methods applied in this master thesis

Details on measurement of logP

The blood-brain barrier provides optimal protection of the brain against pathogens and other potentially toxic substances circulating in the blood, but it is often an obstacle to the development of new drugs that find their site of action in the brain.[39]

An important indicator for the permeability of the blood-brain barrier is the lipophilicity, which is quantified by the logP value and represents an important physicochemical parameter. For an optimal passive brain entry in vivo, the lipophilicity of the test substances should be in a range between 2.0-3.5. Such determination of lipophilicity was performed by HPLC in this master's thesis and was an essential part of the practical work. The extent of solubility of a compound in lipids, oil or non-polar solvents such as Hexane or 1-Octanol is listed under the term lipophilicity. By definition, lipophilicity is the partition coefficient of a non-ionized compound in two immiscible phases (n-Octanol and Water/buffer).[37], [40]

Cell viability

For this master thesis, an MTT assay was performed to exclude a possible toxicity of the substances. The MTT assay is a cytotoxicity test. Cells are treated in vitro with a yellow Tetrazolium salt (MTT; chemically 3-(4,5-dimethylthiazol-2-yl)-2,5-diphenyltetrazolium bromide) to measure their viability or percentage of living cells compared to a control sample. Detection of cell viability using the MTT assay is based on the reduction of the yellow, water-soluble dye to a blue-violet, water-insoluble formazan.

Only viable cells can metabolize MTT to the purple-coloured formazan due to the presence of mitochondrial dehydrogenase enzymes. The reaction scheme can be seen in figure8. Absorption is measured by photometer at a wavelength of 570 nm. The final signal obtained depends, among various aspects, on the incubation time, the number of number of living cells and the metabolic activity of those cells.[41], [42]

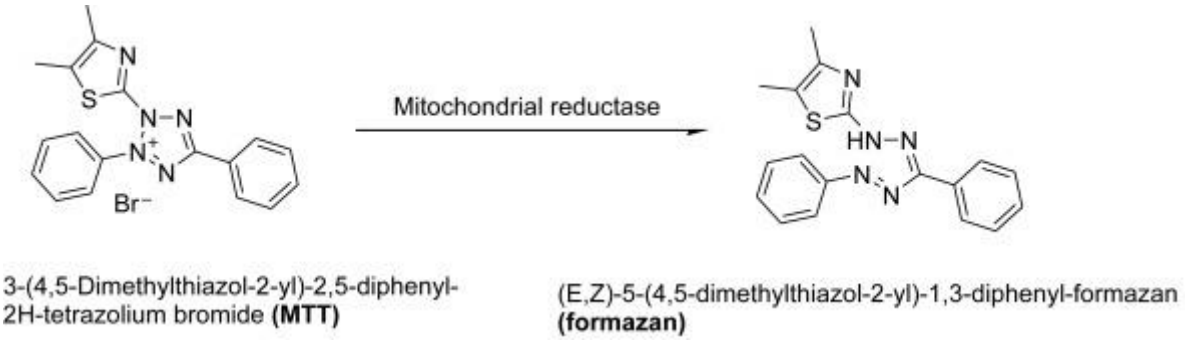

Figure8: Reduction of MTT to insoluble formazan dye by the activity of mitochondrial reductase.[43]

Competitive radioligand binding assay

Receptor-ligand interactions take an essential place in modern pharmaceutical development. There are many of test formats to quantity these interactions. The competitive radioligand binding assay offers the possibility to rapidly perform screening procedures for new ligands. The time savings result from the fact that a variety of conditions and samples can be processed. In general, ligand, radioligand and the receptor-expressing membranes are incubated. Here, the selected radioligand is introduced into the buffer in the presence of displacers or other agents of interest, and ideally binding results so that equilibrium is established between bound and free ligands. After incubation is complete, separation of bound and free radioligand occurs, for example by filtration, centrifugation, adsorption, or precipitation, followed by determination of radioactivity to quantify the bound radioligand. By plotting competitive binding curves, IC_{50} (inhibitory concentration) values and K_i (inhibition constant) values can be determined via the Cheng-Prusoff equation (equation 4).[44]

The strength with a ligand binds to its receptor is described as affinity. Moreover, there is an essential relationship between potency and affinity. The potency reflects the amount of active ingredient required to elicit a particular effect.

Assuming reversible binding, the relationship between ligand, receptor and its complex can be expressed using mass action laws.

Equation 1:

$$[R] + [L^*] \leftrightharpoons [RL^*]$$

The ratio k_{-1} / k_{+1} expresses the K_d (dissociation constant), which is inversely proportional to the ligand affinity to the receptor. This means that the higher the K_d values, the weaker the binding and the lower the affinity.

Equation 2:

$$K_d = \frac{k_{-1}}{k_{+1}} = \frac{[L^*]x[R]}{[RL^*]}$$

At equilibrium, the K_d value provides information about the amount of ligand that saturates 50% of the binding sites.

Equilibrium occurs when the rate at which ligand-receptor complexes are formed and dissociated is identical. At equilibrium the following is valid:

Equation 3:

$$[L][R]k_{on} = [LR]k_{off}$$

By adding a competing analyte, a certain amount of a specifically labelled ligand can be displaced by the analyte of interest. How much is displaced depends on both the concentration and the affinity of the analyte as well as reference compound.

With the aid of variable analyte concentrations, inhibition curves can be prepared from which the IC_{50} value can be calculated.

It should be noted that although different concentrations of the analyte are used, the concentrations of the receptor and the labelled ligand remain constant.

The relationship between IC_{50} value and the affinity constant K_i of the analyte is expressed by the Cheng-Prusoff equation.

Equation 4:

$$IC_{50} = K_i \times \left(1 + \frac{[L^*]}{K_d}\right)$$

Based on this equation, it is possible to calculate the K_i from the IC_{50} in order to compare the affinities of the different ligands to the receptor.[45], [46]

Plotting the bound radioligand semilogarithmically against the log concentration of the unlabelled ligand yields an inverse sigmoid curve, as shown in figure9. While the plateau at the top of the curve corresponds to the amount of bound radioligand in the absence of unlabelled ligand, the lower plateau of the curve illustrates nonspecific binding (NSB). The IC_{50} is defined here as the inflection point of the curve and corresponds to that concentration of unlabelled ligand which displaces 50% of the radioligand between the plateaus.[47], [48]

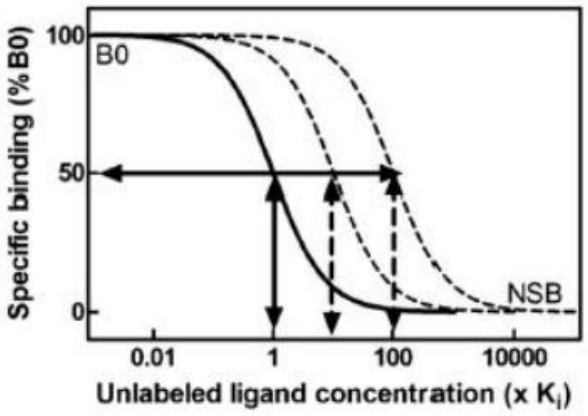

Figure9: Sigmoidal curves of competitive binding.[48]

Aim of this masterthesis

mAChRs play a central role in a variety of neurological diseases. A great deal of research is still being done to develop potential ligands with high affinity and high selectivity for those receptors. Especially in the field of brain research there is a deficit of PET tracers. This deficit often complicates both the diagnosis and subsequent treatment of neurodegenerative diseases. The small selection of available tracers has several backgrounds. A limiting factor in the development of new ligands is the fact that the substances must be able to pass the blood-brain barrier. A major effort of the research is to identify ligands that have high subtype specificity, since the different subtypes of mAChRs have different functions in the brain. The focus of the work was to evaluate the lipophilicity and affinity of a set of twenty-two potential ligands and to rule out possible toxicity. The test substances were rearrangement products of the known M1 antagonist Pirenzepine. RP-HPLC allowed the prediction of logP values and purity. Subsequently, the objectives were to determine the K_i values of the newly synthesized ligands using a competitive radioligand binding assay and to evaluate possible toxicity of the most promising compounds using a cell viability assay.

Materials

- Dimethyl sulfoxide, DMSO (Sigma Aldrich)
- Ethylenediaminetetraacetic acid, EDTA (Sigma Aldrich)
- Geneticin (Life Technologies Limited)
- Gibco Fetal Bovine Serum, FBS (Life Technologies Limited)
- Gibco Dulbecco's Phosphate-Buffered Saline, PBS (Life Technologies Limited)
- L-Glutamine (Life Technologies Limited)
- Medium Gibco F-12 (1x) Nutrient Mixture (Ham) (Life Technologies Limited)
- Methanol (Merck Millipore)
- $MgCl_2$ (Merck Millipore)
- MTT reagent (Sigma Aldrich)
- Na_2HPO_4 (Sigma Aldrich)
- NaH_2PO_4 (Merck Millipore)
- $(NH_4)H_2PO_3$ (Sigma Aldrich)
- [*N*-Methyl-^{3}H]Scopolaminemethylchloride, [*N*-Methyl-^{3}H]NMS (Perkin Elmer, 37 MBq, 2.964 TBq/mmol in 1 mL ethanol)
- Pirenzepine dihydrochloride (Sigma-Aldrich)
- Poly(ethyleneimine) solution, PEI (Fluka Analytical)
- Protease inhibitor P2714 (Sigma Aldrich) dissolved in 10 mL Milli-Q Water and stored at -20 °C
- Tris(hydroxymethyl)aminomethane (Merck Millipore)
- Trypsin 0.05% (Life Technologies Limited)
- Ultima GoldTM (Perkin Elmer)

Methods

Compounds under investigation

22 compounds were investigated in this master thesis for their suitability as potential ligands for the mAChRs. Table3 below shows their structure, molecular weight and chemical formula.

Table3: Compounds of the twenty-two Pirenzepine derivates under investigation, their molecular weight and their chemical formula.

compound	molecular weight and chemical formula	structure
Mima186	297.34 g/mol C17H17N3O	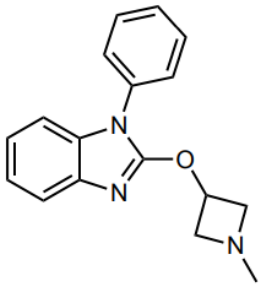
Mima187	346.43 g/mol C21H13N4O	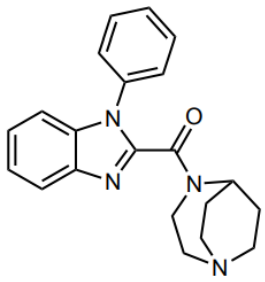
Mima188	346.43 g/mol C21H22N4O	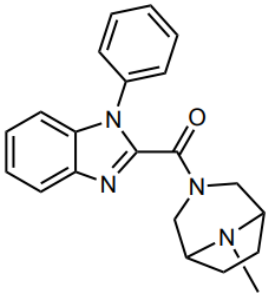

Mima193	321.43 g/mol C19H23N5	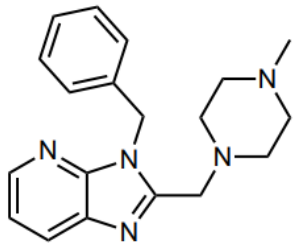
Mima194	333.44 g/mol C20H11N2O	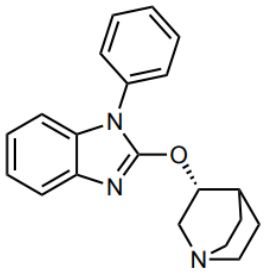
Mima195	347.42 g/mol C21H21N3O2	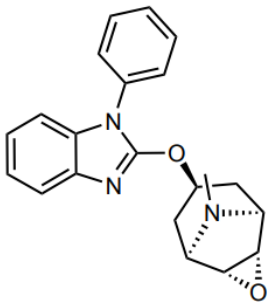
Jela2	332.45 g/mol C21H22N4	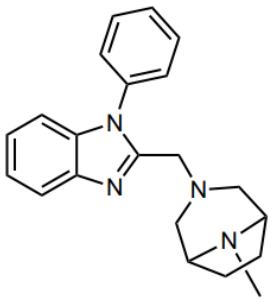
Jela5	336.44 g/mol C20H24N4O	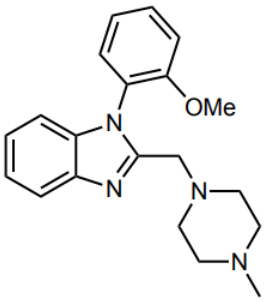

Jela11	297.33 g/mol C17H16F1N3O	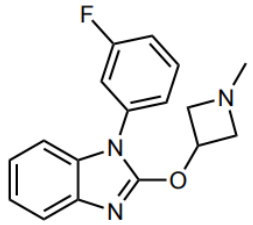
Jela12	351.43 g/mol C21H21F1N2O	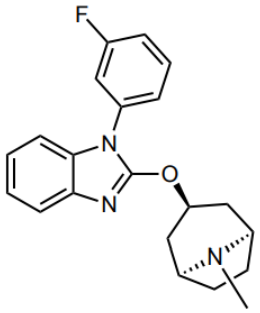
Jela17	306.41 g/mol C19H21N4	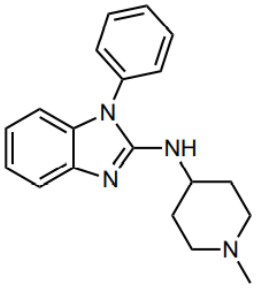
Jela19	320.44 g/mol C20H23N4	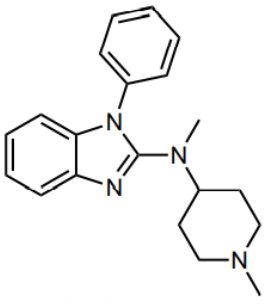
Jela20	306.41 g/mol C19H21N4	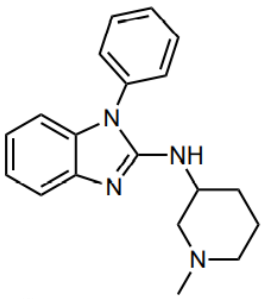

Jela21	336.48 g/mol C21H28N4	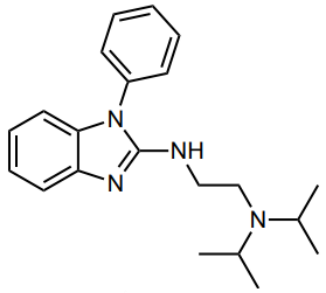
Jela22	333.44 g/mol C19H24N3O	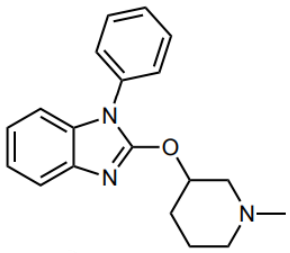
Ledza18	320.44 g/mol C20H24N4	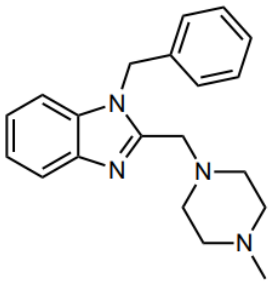
Ledza22	307.40 g/mol C19H21N3O	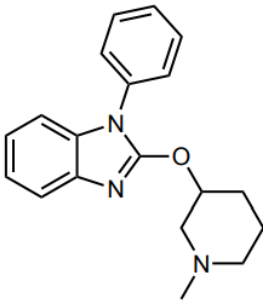
Ledza23	293.37 g/mol C18H19N3O	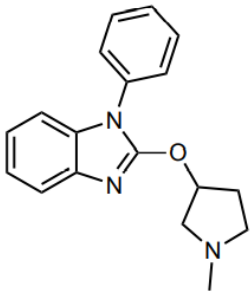

Ledza24	307.40 g/mol C19H21N3O	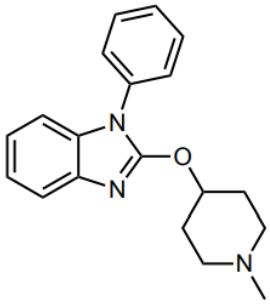
Ledza36	320.44 g/mol C20H24N4	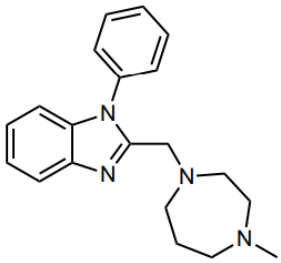
Ledza41	351.41 g/mol C19H21N5O2	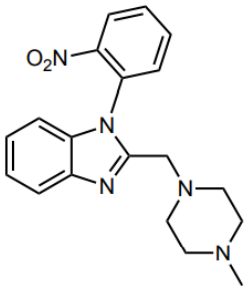
Ledza42	331.42 g/mol C20H21N5	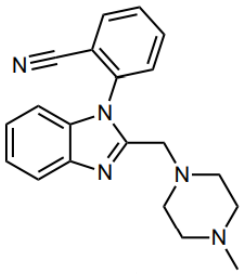

Equipment

• Brandel Cell Harvester

• HIDEX 300 SL Automatic TDCR Liquid Scintillation Counter

• HPLC consisting of: column: XSelect® HSST 33.5 µm, 4.6 x 100 mm, autosampler: Agilent Technologies 1100 series, pump: Agilent Technologies 1200

series, diode array detector (series 1100), radiodetector (Ramona, Elysia-Raytest)

• Sorvall Ultracentrifuge Combi

LogP values and purity of compounds under investigation via HPLC

An Agilent HPLC system consisting of an autoinjector, a pump, a diode array detector and a radio detector was used to analyze the logP values of all the compounds studied. The components of the mobile phase were as follows: Methanol and Sodium phosphate dibasic, Water from the Milli-Q® Integral Water Purification System. A gradient program was used, initially starting with 10% Methanol and 90% Sodium phosphate buffer, increasing to 100% Methanol at 9.4 min with a flow rate of 1.5 mL/min, and ending with initial conditions after 13 min. The stationary phase was an Octadecyl poly(vinyl alcohol) 50 (ODP) column (20 × 4 mm, 5 µm). 5 µL of the test substance was mixed with 25 µL of a logP cocktail. The logP cocktail consisted of the following components and reference compounds: Methanol, 0.1 mg/mL Triphenylene and 0.01 mg/mL Toluene, and 20 µL distilled Water. These conditions eventually resulted in a pressure of 20 bar. Wavelengths of 254 nm and 285 nm were chosen for the measurement. The logP value was calculated from the retention time of the analyte and the reference compounds Triphenylene and Toluene using logP values known from the literature. The formulas for the calculation were used as described by Vraka et al.[37]

The Agilent HPLC system described above was also used for the determination of purity. Methanol and 10 mM dibasic Sodium phosphate buffer pH 7.4 and Water from the Milli-Q® Integral Water Purification System were chosen as the mobile phase. The stationary phase was an ODP (Octadecyl poly(vinyl alcohol) 50 column (20 × 4 mm, 5 µm), as in the determination of logP values. The following conditions were chosen: Gradient elution, starting with 10% Methanol and 90% Sodium phosphate buffer to 100% Methanol in 9.4 min with a flow rate of 1.0 mL/min, at an injection volume of 5 µL and ending with the initial conditions after 15 min.

In addition, an isocratic run was performed with Mima186, Mima187, Mima188, Mima193, and Mima194. For this, the logP-HPLC method described above without addition of Toluene and Triphenylene was chosen on an XSelectTM (HSS T3, 3.5 µm, 100 × 4.6 mm) stationary phase at a flow of 1 mL/min and an injection volume of 5 µL. The wavelength was set to 216 nm for both methods (gradient and isocratic).

All analytes were prepared for both gradient and isocratic modes as follows. The various compounds were dissolved in DMSO at a concentration of 10 mM. 5 µL of the test compound was mixed with 45 µL of distilled Water in an HPLC tube and then added to the instrument. Purity was expressed as the area of the product peak relative to the total area of all peaks as a percentage.[49][37] Those compounds with a purity of > 95% were considered for further testing.

Cell Culture

For the experiments CHO-K1 (chinese hamster ovary) cells stably transfected with human muscarinic receptors M1-M5 were obtained from Missouri University of Science and Technology cDNA Resource Center (Cell Catalog#: CEM1000000, CEM2000000, CEM3000000, CEM4000000, CEM5000000). The cells were cultured in F-12 nutrient mixture media (Ham) with 10% Fetal bovine serum (FBS) and 0.5% Geneticin. T175 cell culture flasks with a surface area of 175 cm^2 were suitable for the experiments. The cells were stored in a cell incubator under humified atmosphere containing 5% CO_2.

Thawing

To thaw frozen cells, a Falcon tube with 5 mL complete medium was prepared. As soon as the cell suspension was thawed in the cryovial, it was quickly transferred into the prepared Falcon tube. The cells were then centrifuged for about 5 min at 1200 rpm. Then the supernatant was removed, and the pellet was resuspended in 1 mL medium. The suspension was finally transferred to a new 75 cm^2 cell culture flask containing 12.5 mL growth medium and allowed to resume exponential growth.

Freezing

For freezing, the cells were divided as described indicated below and then the suspension was transferred to a falcon tube and centrifuged for 5 min at 1200 rpm. Meanwhile a freezing medium was prepared by adding 10% DMSO to the complete

medium. After centrifugation, the supernatant was removed, and the cell pellet formed at the bottom was resuspended in the freshly prepared freezing medium. The cell suspension was then aliquoted into the tubes with a volume of 1 mL each. The tubes were placed in Mr. Frosty™ and stored overnight at -80°C to achieve the optimal cooling rate of nearly 1°C/min for cell preservation. For long-term storage, the cells are transferred into liquid nitrogen.

Splitting

In order to keep the cells at exponential growth, cells were examined several times a week and had to be splitted once they reached a confluence of > 80-90%. For this, the old medium was removed, and the cells were washed once with 7 mL Gibco® Dulbecco's phosphate buffered saline (DPBS). Then 2 mL Trypsin 0.05% (Life Technologies Limited) was added to detach the cells from the bottom of the flask. The cell culture flask was placed for approx. 5 min in the incubator to achieve an ideal detachment of the cells. Complete detachment was checked under the microscope. By adding double the amount of medium, the reaction was stopped, and the cells were separated from each other by repeated pipetting. After everything was well suspended, an aliquot was removed and transferred to a cell culture flask filled with fresh medium in order to gain ideal growing conditions again.

Cell counting

To determine the number of cells for further experiments an aliquot of the cell suspension which was produced in course of the splitting procedure was used. For this, about 18 µL of the cell suspension were carefully pipetted along the edge of the cover glass of the Neubauer haemocytometer until the cover glass was finally completely filled. The suspension was drawn inside the haemocytometer by capillary action. Before counting, the entire grid of lines must be viewed at a low magnification and checked to see if the cells are evenly distributed across the squares. If there is an uneven distribution, the particle suspension should be shaken again and reintroduced into the counting chamber. The cells in the four large squares were counted under the microscope. The arrow drawn in figure10 shows the procedure for cell counting.

To avoid counting errors, it is important not to double count cells lying on border lines. For that reason, it is common to count only the cells on two boundary lines (e.g. top and left) when counting a square and not the cells on the other two lines.

The average of the counted squares was then determined, and the concentration derived from this by equation 5.

Equation 5: $$\frac{\text{counted cells}}{\text{number of counted squares}} = \text{x} \times 10^4 \text{c/mL}$$

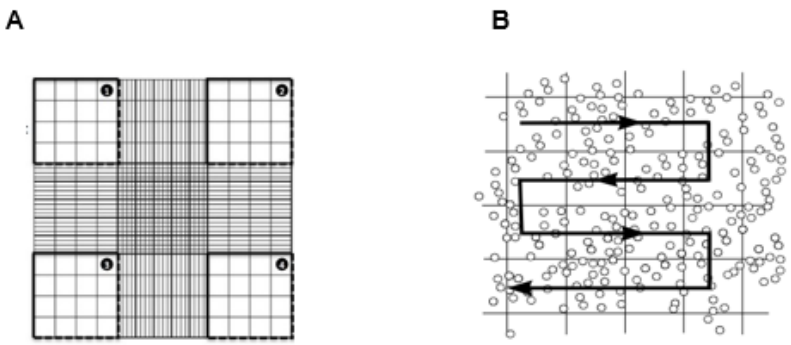

Figure10: Cell counting with a Hemocytometer: (A) Depiction of the grid of a Neubauer chamber. (B) The cells of each of the four counting grids were counted via the shown procedure.[50] [51]

MTT assay

For the MTT assay, CHO M1 cells were seeded in a 96 well plate in a concentration of 2000 cells/well. To obtain cell suspension with a concentration of 2000 cells/well, equation 6 was used. 100 µL of this suspension was placed per well. A triplicate determination was performed so that a total of 60 wells were filled with the cell suspension.

Equation 6:

$$c_1 \cdot V_1 = c_2 \cdot V_2$$

c_1: number of cells per mL calculated during counting

V_1: needed volume of cell suspension

c_2: desired number of cells per well

V_2: needed volume of medium

After the seeding the cells were incubated with 37°C and 5% CO_2 for 24 h, in order to let the cells attach at the bottom of the well plate. After 24 h the test substances were added. First, stock solutions of the two test substances, Mima194 and Mima187 had to be prepared. For each stock solution a volume of 800 µL and a concentration of 2 mM was chosen to achieve a concentration of less than 1% DMSO and to avoid cell damage.

The highest concentration of the dilution series was chosen to be twice the final concentration. From the known required volume (V), concentration (c) of the drug stock solution and molecular weight (M) of the compound, the required amount of substance (m) could be derived using the following equations:

Equation 7 and 8:

$$c = \frac{n}{V} \qquad n = \frac{m}{M}$$

A serial dilution of 1:2, starting with the highest concentration, was performed to obtain nine different concentrations (1000 µM, 500 µM, 250 µM, 125 µM, 62,5 µM, 31.25 µM, 15.63 µM, 7.82 µM 3.91 µM). An overview of the different concentrations is given in table4.

Table4: Overview of the nine concentrations used in the MTT assay.

Well number	3	4	5	6	7	8	9	10	11
Concentration in µM	3.9	7.82	15.63	31.25	62.5	125	250	500	1000

After the serial dilution was completed the addition of the test substances (Mima187, Mima194) could be started. For this purpose, well B2-D2 of the 96 well plate was filled with 100 µL growth media only as negative control in triplicates. The initial step was the lowest dilution. Well number 3 was filled with triplicates of the next higher dilution and the same procedure was performed with the other well numbers, so that the concentration of the added drugs increased from left to right. (figure11)

After 72 hours a MTT working solution was prepared by adding 1 mL MTT stock solution (concentration: 5 mg/mL MTT in PBS) to 6 mL culture medium. The medium covering the cells in the 96 well plate was discarded and 100 µL MTT working solution was pipetted into each well, followed by an incubation period of 4 hours at 37 °C. The MTT working solution was then removed and 100 µL DMSO was added. The plate was then measured at a wavelength of 570 nm with a reference wavelength of 690 nm. Pirenzepine and the Pirenzepine-rearrangement product (figure7) served as controls using the same concentrations. The IC_{50} was calculated using GraphPad Prism.

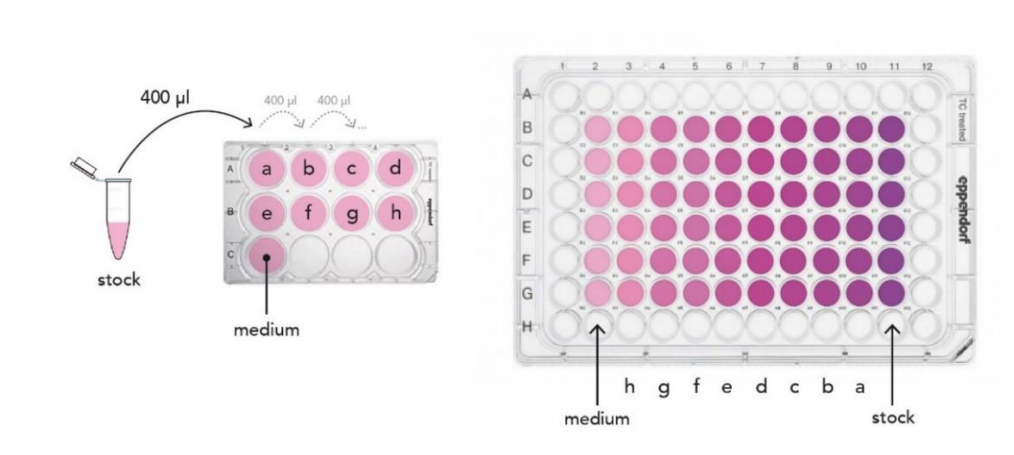

Figure11: Pipetting scheme and dilution of the MTT assay on a 96 well plate.

Harvester experiments

Membrane Preparation

For membrane preparation, CHO-M1, CHO-M2, CHO-M3, CHO-M4, CHO-M5 cells transfected with the desired subtype were cultured in ten T175 flasks until at least 80% confluence was achieved. First, the old medium was removed from the flasks and the cells were washed with 7 mL of DPBS. Then, 2 mL of ice-cold buffer (10 mM Tris/HCl and 1 mM EDTA at pH 7.4) was added before detaching the cells with a cell scraper. The cell suspension was transferred to five 5 mL Eppendorf tubes already filled with 400 µL protease inhibitor.

The contents of the Eppendorf tubes were homogenized by forcing them through an insulin syringe. First, they were centrifuged at 1000 g for 10 min at 4 °C.

Then, the supernatant was transferred to SETON tubes and centrifuged at 100 000 g for 40 min at 4 °C. The supernatant was removed, and the pellet was dissolved in 50 mM Tris/HCl buffer pH 7.4. The membrane solution was then transferred to cryotubes and stored at -80 °C.

Competitive binding assay

First, the compounds were dissolved in DMSO. 5 µL of different concentrations (each pipetted in triplicate), pure DMSO to evaluate the maximum binding potential (blank) and a 100 µM solution of Scopolamine in DMSO to measure the non-specific binding (positive control) were pipetted into the test tubes. For this replacement experiment the radioligand [*N*-Methyl-^{3}H]scopolaminemethylchloride was dissolved in different concentrations according to the expression level of the receptor subtype in a buffer solution of 50 mM Tris, 10 mM $MgCl_2$ and 1 mM EDTA in distilled Water with a pH of 7.4. The most efficient concentrations of radioland for M1-M5 were 0.2 nM, 0.3 nM, 0.8 nM, 0.2 nM, and 1.0 nM. (See table5)

Table5: Concentration of radioligand and amount of membrane suspension used in harvester experiments.

	M1	**M2**	**M3**	**M4**	**M5**
concentration of radioligand [nM]	0.2	0.3	0.8	0.2	1.0
amount of membrane suspension used [µL]	90 – 150	150 – 400	90 – 200	150 -300	150 – 200

The respective membrane suspension was suspended in the assay buffer. Subsequently, 445 µL of this solution was added to the tubes and then incubated for 90 min at room temperature. A GF/B filter was used for the filtration. For this purpose, the filter was soaked with a 0.5% solution of PEI in distilled Water. First the Cell Harvester (shown in figure12) was washed with washing buffer containing 50 mM Tris in distilled Water at pH 7.4. After incubation, filtration was performed with the prepared Cell Harvester and the test tubes were washed two times with the ice-cold wash buffer. The filter was then stamped out and 2 mL of the scintillation cocktail (Ultima Gold™, high flashpoint LSC cocktail, PerkinElmer) was added.

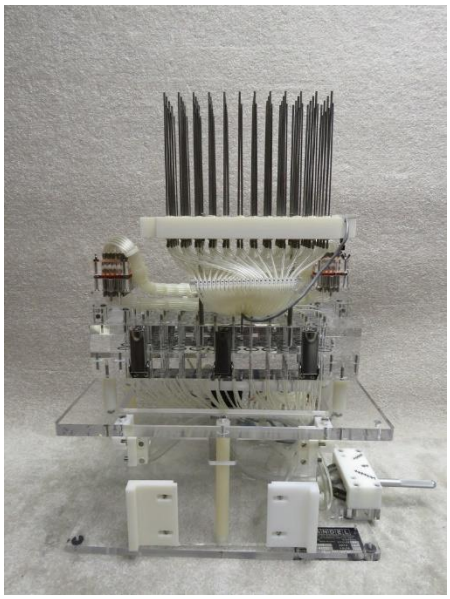

Figure12: Cell harvester.[52]

The test tubes were shaken for 10 minutes and the filter disks were counted using a 300 SL Automatic TDCR liquid Scintillation Counter (HIDEX) in CPM mode. The counting time lasted 60 seconds and the activity type set to low. Subsequently, the obtained counts per minute (cpm) were analyzed using GraphPad Prism 6. The cpm were charted against the logarithms of the concentrations so that the IC_{50} could be determined using non-linear regression. The IC_{50} value was then converted to K_i using the Cheng-Prusoff equation (equation4). Using GraphPad Prism 6 software, the data collected with the beta counter (cpm) were plotted against the logarithms of the concentrations of the tested compounds.

The K_i of potential radioligands needs to be in the nanomolar range to be considered as a possible PET tracer. Therefore, a cut-off was set at a concentration corresponding to a K_i of 1 µM. The K_d values of the radioligand are required for the calculation of K_i values, and the K_d values of radioligands of 0.17 nM, 0.15 nM, 0.16 nM, 0.07 nM, and 0.16 nM were determined for M1-M5. (See table6).

Table6: Literature K_d values of [*N*-Methyl-^{3}H]scopolaminemethylchloride.

	M1	**M2**	**M3**	**M4**	**M5**
K_d [nM]	0.17	0.15	0.16	0.07	0.16

Results and discussion

Purity determination

To guarantee that the biological effect is due to the compound itself and not caused by potential impurities, a purity test was carried out using RP-HPLC. A threshold of at least 95% was defined in our group for a compound to be considered as pure and to be forwarded to further biological screening. In total, 22 compounds were tested for their purity. (table7) About 90% of the compounds showed >95% purity. Mima195 and Jela5 did not comply with the desired purity requirements and were therefore excluded from further investigations. For Mima186, Mima187, Mima188, Mima193, and Mima194, both a gradient method and an isocratic run were performed to more accurately assess purity and obtain the ideal baseline conditions. The results obtained from the isocratic run were in agreement with those obtained from the gradient elution. These compounds which did not comply with the requirements are highlighted in gray in table7 below.

Lipophilicity determination based on logP values

The measurement of the 22 compounds showed a logP value between 1.47 and 3.64 (table6). The four most lipophilic compounds are, in descending order: Jela21 (3.64), Jela12 (3.09), Jela22 (3.05) and Mima195 (3.04). Those structures are furnished with the identical 1-Phenyl-1,3-benzodiazole backbone. However, differences arise from two substituents. All four compounds bear a comparable N-Benzylgroup, whereas the second substituent vary greatly. In particular, the results for Jela12, Jela22 and Mima195 are structurally closely related with the second substituent being an ether fragment including cyclic amines. The introduction of a fluorine substituent on the N-Benzylgroup had only a minor effect on the logP value. The exchange from an ether to an amine coupling including a linear aliphatic amine compared to a cyclic one had a greater impact as seen for Jela21.

The least lipophilic compounds are as follows in decreasing order: Ledza36 (1.97), Mima193 (1.61), Mima187 (1.47) and Ledza42 (1.48). Again, all four compounds consist of the similar backbone derived from the previously published Pirenzepine rearrangement.

The two residues of Mima187, Ledza36 and Ledza42 consist of a benzyl moiety and methylene- or amide-bridged cyclic amines, whereas Mima193 is furnished with a Phenyl group. The change from Benzyl- to a Phenyl group raised the logP value from 1.48 to 1.61. Changing the six-membered cyclic amines to a seven-membered one increased the lipophilicity further up to a value of 1.97. The exchange from a methylene-bridge to an amide-bridge, however, decreased the logP value again.

According to the Lipinski rule, only compounds can cross *via* cellular membranes, including the blood-brain barrier, with logP value in a range between 2.0 and 3.5. In general, 75% of the here tested compounds are in accordance with the Lipinskis rule. Mima187, Mima193, Ledza36 and Ledza42 would be considered too hydrophilic for passive diffusion, whereas Jela21 would be too lipophilic and therefore the unspecific binding would be too high. Nevertheless, the Lipinski rule of five is only an estimate and would not be able to predict the actual CNS penetration. The purity and logP values of the gradient method are listed in table7.

Table7: Overview on the measured purity (gradient method) and chromatographic evaluated logP values from 22 compounds under investigation.

compound	purity	logP
Mima186	100±0	2.65±0.07
Mima187	98.77±0.29	1.47±0.24
Mima188	96.44±0.33	1.88±0.33
Mima193	96.14±0.55	1.61±0.22
Mima194	99.95±0.04	2.96±0.02
Mima195	93.36±0.06	3.04±0.01
Jela2	99.73±0.19	2.3±0.12
Jela5	94.99±0.15	2.07±0.15
Jela11	99.79±0.15	2.88±0.03
Jela12	99.30±0.03	3.09±0.02
Jela17	99.81±0.02	2.31±0.12
Jela19	99.39±0.24	2.68±0.06
Jela20	99.72±0.04	2.61±0.07
Jela21	98.47±0.62	3.64±0.08
Jela22	100±0	3.05±0.01
Ledza18	97.73±0.15	2.06±0.15
Ledza22	99.92±0.06	3.20±0.02
Ledza23	99.93±0.05	2.81±0.04
Ledza24	100±0	2.94±0.03
Ledza36	99.18±0.02	1.97±0.17
Ledza41	100±0	2.02±0.16
Ledza42	99.11±0.63	1.48±0.24

Cell viability

As high cell toxicity would interfere with the subsequent affinity determination, an MTT assay was performed in concentrations range from 1000 - 3.91 µM for Mima187 and Mima194, whereas Pirenzepine and the identified Pirenzepine rearrangement product serve as control. In this context, the IC_{50} value defines the concentration at which cell viability decreased by 50%.

The control compounds Pirenzepine and the rearranged Pirenzepine as well as Mima187 had no influence on the cell viability in the tested concentration range. Mima194 showed an IC_{50} value of 150 µM, which indicated a low to moderate toxicity. However, as only compounds with nanomolar affinity are interesting in regard of the here envisaged drug development process, no interference of toxicity for the further experiments was expected.[35]

The dose-response curves are shown in figure13 and the calculated IC_{50} values are depicted in table8.

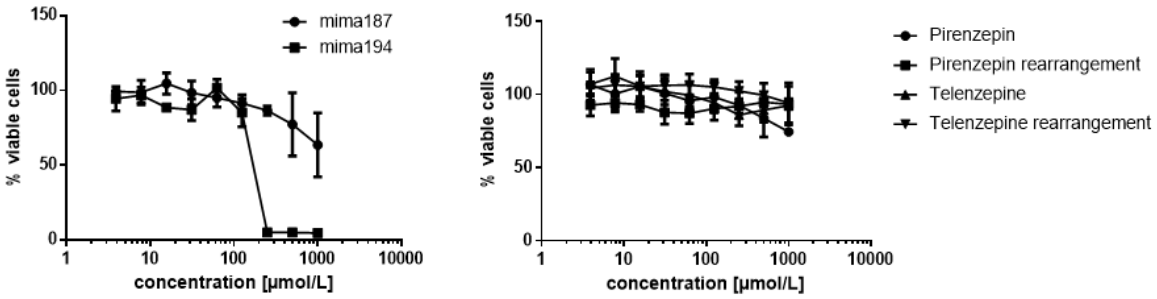

Figure13: Concentration-effect curves as determined by the MTT assays.

Table8: Calculated IC_{50} values of the substances.

compound	**IC_{50} [µmol/L]**
Mima187	>1000
Mima194	148±18
Pirenzepine	>1000
Pirenzepine rearrangement	>1000

Competitive binding assay – Screening

In a next step, the compounds were tested for a single-concentration binding affinity at a cut-off concentration of 1 µM for all mAChR subtypes. The screening process was chosen to increase the testing speed for a high number of compounds. These compounds are listed in table3. The further assumptions are mainly based on the percentual displacement and can only offer a prediction of subtype selectivity. Table9 shows the percentual displacement on the different subtypes. In order to confirm the affinity and subtype selectivity the most promising compounds were tested for their K_i values.

More than 60% of the compounds showed displacement of > 50% for all subtypes, which would forecast a K_i value in the nanomolar range. Mima193 did not show the required high displacement to result in K_i values in the nanomolar range for any of the 5 subtypes to be considered as a PET radiotracer. The displacement here was below 30% for all 5 subtypes. Jela11 only reached a displacement of > 50% for the M5 subtype and therefore it is highly unlikely, that the nanomolar K_i will be reached for any of the subtypes.

An intermediate displacement was found for Ledza18, Ledza22, Jela 20, Jela 21, Mima 188 and Mima187. Mima188 reached the required displacement only for M1, M4 and M5. The displacement was about 76% for Mima187 for the M1 subtype. For the remaining subtypes M2-M4, displacements below 60% were obtained, which overall suggests that this substance shows intermediate affinity. The two Ledza compounds showed a slightly preference for M4 and M5 subtype, whereas the two Jela compounds offered the highest displacement on M1.

Mima194, Jela12, Jela17, Jela19, Ledza23 and Ledza24 showed the best overall displacement in this screening and are therefore considered as the most promising compounds. Here, the displacement percentages for all subtypes were over 80%.

Those compounds which showed a displacement of at least 50% against [*N*-Methyl-^{3}H]NMS would be of particular interest for determination of the K_i value. One of the most promising compounds, Mima194, and one intermediate one as reference, Mima187, were selected for the subsequent determination of their K_i value for all five subtypes.

Table9: Percentual displacement on the different subtypes shown by the tested structures.

compound	M1	M2	M3	M4	M5
Mima187	76.74±4.71	53.68±10.49	81.15±1.79	61.22±3.99	77.04±4.30
Mima188	64.67±5.66	43.93±14.42	32.00±1.15	52.91±1.10	58.94±5.64
Mima193	24.35±8.97	26.42±1.51	21.40±4.17	24.03±7.26	33.64±7.37
Mima194	101.07±2.46	96.58±1.86	101.66±3.39	97.58±0.76	98.88±1.02
Jela2	80.96±7.19	65.47±10.45	60.51±0.63	79.08±3.65	76.04±3.87
Jela11	40.27±6.07	31.78±6.56	33.03±3.30	35.04±6.44	53.71±4.56
Jela12	89.83±3.14	85.99±13.28	99.39±4.12	91.30±0.68	95.66±2.40
Jela17	95.86±2.26	91.25±1.32	89.08±1.16	93.95±1.93	89.09±2.27
Jela19	97.49±2.01	86.18±0.76	78.78±1.79	93.26±1.10	90.26±2.54
Jela20	73.69±6.15	50.16±0.81	33.42±4.94	67.52±2.84	61.77±2.22
Jela21	73.82±2.85	66.79±0.58	23.38±1.42	62.61±1.29	63.39±2.25
Jela22	98.36±2.69	100.85±0.94	95.13±0.12	101.22±1.61	93.31±6.69
Ledza18	52.08±3.81	62.86±19.24	50.37±1.53	71.17±2.07	74.26±7.21
Ledza22	79.06±4.36	64.27±19.55	72.41±3.22	84.84±0.76	86.88±1.76
Ledza23	90.57±2.06	85.11±1.06	87.73±1.05	92.75±1.07	92.98±2.24
Ledza24	95.54±1.11	93.65±2.36	97.03±1.44	97.36±1.35	89.46±3.04
Ledza36	94.50±2.00	70.95±0.46	71.09±0.73	88.15±2.64	85.34±3.75
Ledza41	94.25±1.62	71.86±1.47	42.18±1.79	84.22±0.19	83.33±0.83
Ledza42	96.14±0.87	85.56±2.62	53.53±7.70	90.46±2.60	85.13±3.76

Competitive binding assay – Ki values

The K_i value of Mima187 and Mima194 against all five mAChR subtypes were determined using a competitive radioligand binding assay. Based on literature, K_i values around 3-50 nM are considered relevant for potential mAChR PET ligands. For our testing regime, K_i values above 50 nM indicates low affinity. [28]

Based on the screening results obtained previously, Mima194 was tested for its K_i on all five mAChR subtypes, while Mima187 was tested only on the M1 mAChR. Here, [*N*-Methyl-^{3}H]NMS was used radioligand to identify the competitive binding. The K_i values are listed in the table10 below.

Table10: K_i values as determined by an competitive binding assay applying cell membranes expressing the respective mAChR subtype and [*N*-Methyl-^{3}H]NMS as radioligand.

compound	K_i [µM] M1	K_i [µM] M2	K_i [µM] M3	K_i [µM] M4	K_i [µM] M5
Mima187	0.192±0.046	>1	>1	>1	>1
Mima194	0.016±0.003	0.070±0.028	0.004±0.002	0.009±0.001	0.0026±0.0007

Mima187 showed an affinity of 192 ± 46 nM toward the M1 subtype, which can be considered as too high for further in vivo evaluation. The subtype selectivity can only be estimated, as the exact K_i values were not measured. Of interest here is still the subtype specificity. Since Mima187 shows affinity in the desired nanomolar range only for the M1 subtype, the compounds structure would be of interest for further structural improvement for the development of a selective M1 tracer. Regarding the fact that the affinity for the other subtypes (M2-M5) does not meet the requirements for the development of a PET tracer, this compound would be suitable as a potential therapeutic agent from this point of view.

Mima194 showed inhibition constants in the low nanomolar range against all mAChR subtypes. As expected, Mima194 is more affine to all subtypes of mAChR than Mima187. This highlights the efficacy of the screening process. The binding affinity of Mima194 to M3, M4 and M5 can be judged as excellent, as the K_i values here are

below 10 nM. Towards M1, Mima194 has a good binding affinity with a K_i value of 16.1 nM whereas the K_i value towards the M2 subtype indicates a rather lower affinity. Since Mima194 has affinity in the nanomolar range for all subtypes, this compound will be forwarded to further in vivo testing. The structures of Mima187 and Mima194 are shown in figure14.

A **B**

Figure14: Structure of Pirenzepine derivates: (A) Mima187, (B) Mima194.

Looking at the structures more closely, a strong structural similarity is striking for Mima197 and Mima194. While Mima187 has an amide bridge connecting the backbone with the cyclic amine residue, the cyclic amine of Mima194 was connected via an ether group. The exchange of the amide to the ether lowers the lipophilicity as well as the availability of hydrogen bond acceptors. Also sterical hindrance could be a reason for the lower affinity of Mima187 compared to Mima194, as the cyclic amine was exchanged from a seven- to a six membered ring. Figure15 shows the results of the competitive radioligand binding assay for Mima187 and Mima194.

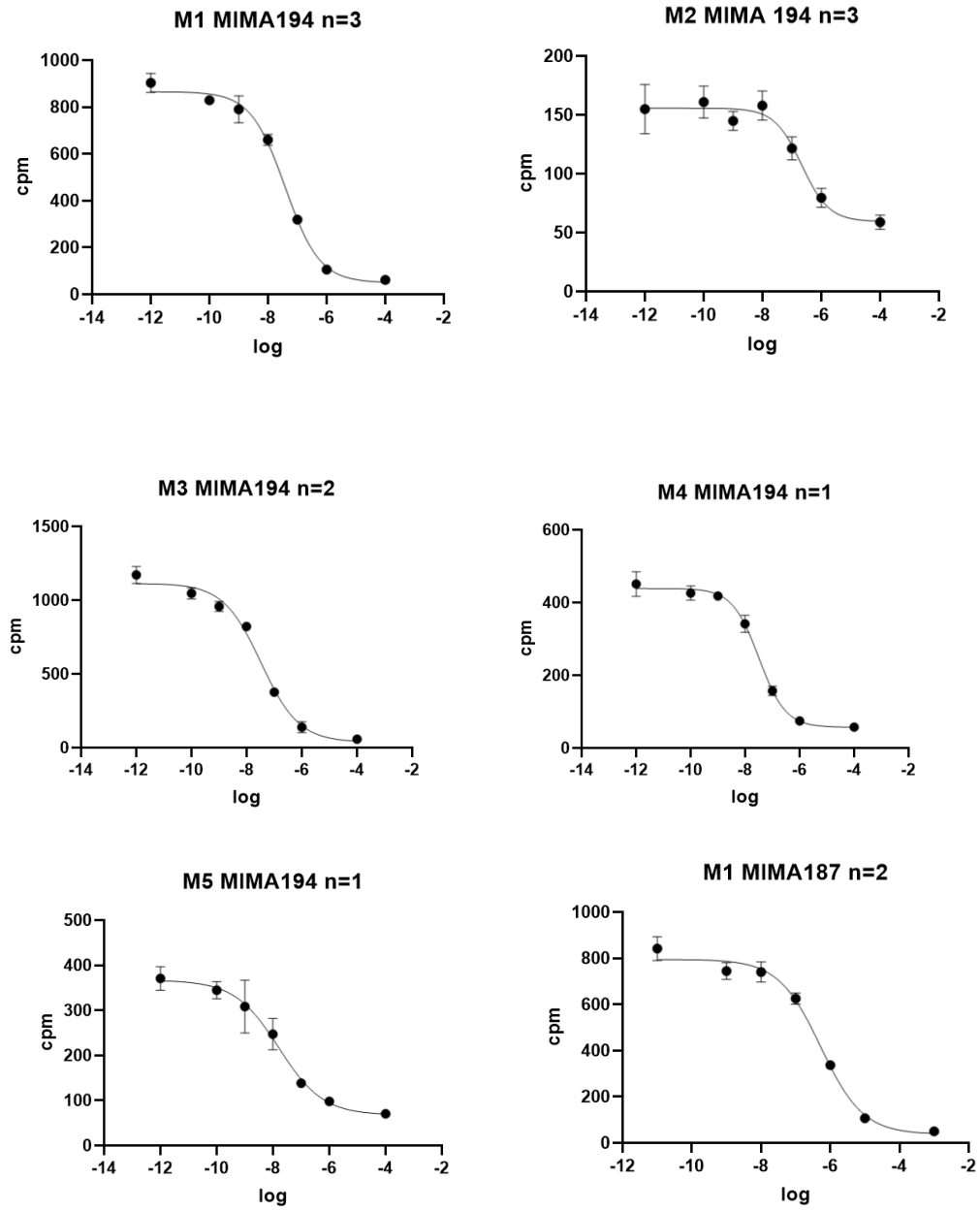

Figure15: Results of a competitive radioligand binding assay for the most promising compound Mima194, using membranes expressing the respective mAChR subtypes.

Structural assumption and outlook

With the exception of Mima187, Mima194 and Jela21, the structures have a free Methyl group, which is excellent for carbon-11 labelling.

It is also worth mentioning that Jela11 and Jela12 have a fluorine group and a free Methyl group in their structures, which makes the compounds particularly interesting for PET tracers, since radioactive labelling with both carbon-11 and Fluorine-18 is possible here.

The most promising compound Mima194 proved to be very difficult to label, as neither a Methyl group nor a Fluorine group is present here. Structural changes would be necessary here to optimally introduce radiolabelling.

For example, a single Hydrogen could be substituted with a Fuorine, allowing Flour-18 labelling.

Conclusion

In this master thesis twentytwo potential ligands for the muscarinic acetylcholine receptor were investigated in terms of physico-chemical parameters, cell viability and affinity towards the target. The idea was to identify ligands with optimal affinity and ideally with high subtype selectivity to set a new milestone in PET tracer development. First of all, a quality test of the potential ligands was performed to ensure their purity. The threshold value was set to at least 95% purity. Two substances (Mima195, Jela5) did not meet this requirement and where further purified before subsequent biological examination. Next, the lipophilicity of the compounds was evaluated by measuring the logP value. Five compounds of the test series failed to overcome this hurdle (Mima187, Mima193, Ledza36 and Ledza42). Still Mima187 was tested for K_i. In the subsequent screening, the displacement of the compounds was determined at a concentration corresponding to a K_i-value of 1000 nM. In those affinity measurements, over 60% of the screened compounds were found to be potential hits. Mima194, Jela12, Jela17, Jela19, Ledza23 and Ledza24 showed the best overall displacement in this screening. Here, the percentages for all subtypes were over 80%. Only one compound, Jela11, showed slight selectivity for the M5 receptor. For the remaining compounds, no selectivity for only one receptor subtype could be detected. The most promising compound and one intermediate one from the screening were tested for their K_i-value to provide evidence of subtype selectivity. Of particular interest were Mima187 and Mima194, with which a toxicity test was also performed. Mima187 showed a slight selectivity towards the M1 subtype in the K_i measurement. Mima194 showed inhibition constants in the low nanomolar range against all mAChR subtypes. It should be noted here that the binding affinity to M3, M4, and M5 are judged to be excellent. The results of the MTT assay showed that both Mima187 and Mima194 were found non-toxic. For Mima187, no toxicity occurred in the nanomolar range. For Mima194, the value was approximately 150 µM, but since the subsequently measured K_i value is lower by a factor of 1000, the substance can be considered non-toxic. It can be clearly seen that the screening method can be used to rapidly screen a large amount of potential ligands, thereby identifying those compounds that are promising for subsequent accurate K_i measurement. Thus, screening offers significant time and cost reduction in drug discovery.

List of Abbreviations

AC: Adenylate cyclase

AD: Alzheimer`s disease

cAMP: Cyclic Adenosine Monophosphate

CHO cells: Chinese hamster ovary cells

CNS: central nervous system

cpm: counts per minute

[^{11}C]PIB: Pittsburgh compound B

DAG: Diacyglycerol

DMSO: Dimethyl sulfoxide

[^{11}C]DASB: 3-amino-4-(2-dimethylaminomethylphenylsulfanyl)-benzonitrile

DPBS: Dulbecco's phosphate-buffered saline

DTNB: 5,5'-Dithiobis-(2-nitrobenzoic acid)

EDTA: Ethylenediamine tetraacetic acid

FBS: Gibco Fetal Bovine Serum

2-[^{18}F]FDG: 2-[18F]fluoro-2- deoxy-D-glucose

[^{18}F]-FDOPA: 6-fluoro-(18F)-L-3,4-dihydroxyphenylalanine

HPLC: High-performance liquid chromatography

IC_{50}: inhibitory concentration

IP_3: Inositol-1,4,5-trisphosphate

K_d: dissociation constant

K_i: inhibition constant

mAChR: Muscarinic acetylcholine receptor

MTT: 3-(4,5-dimethylthiazol-2-yl)-2,5-diphenyltetrazolium bromide

[*N*-Methyl-^{3}H]NMS: [N-Methyl-^{3}H]scopolaminemethylchloride

ODP: Octadecyl-polyvinyl alcohol

PD: Parkinson's disease

PEI: Polyethylenimine

PET: Positron emission tomography

PLC: Phospholipase-C

PKC: Protein kinase C

RP-HPLC: Reversed phase high-performance liquid chromatography

TRIS: Tris(hydroxymethyl)aminomethane

List of Tables

List of Figures

References

[1] S. Duong, T. Patel, and F. Chang, “Dementia: What pharmacists need to know,” *Can. Pharm. J.*, vol. 150, no. 2, pp. 118–129, 2017, doi: 10.1177/1715163517690745.

[2] D. J. Selkoe, “Alzheimer ’ s disease : Genes , proteins , and therapy,” vol. 81, no. 2001, p. 4110, 2018.

[3] J. Coyle, D. Price, and M. DeLong, “Alzheimer’s Disease: A Disorder of Cortical Cholinergic Innervation,” *Science (80-.).*, vol. 219, no. 4589, 1983.

[4] A. M. Palmer, “Pharmacotherapy for Alzheimer’s disease: Progress and prospects,” *Trends Pharmacol. Sci.*, vol. 23, no. 9, pp. 426–433, 2002, doi: 10.1016/S0165-6147(02)02056-4.

[5] D. S.-M. and G. D. R. Marianne Chapleau, Leonardo Iaccarino, “The Role of Amyloid PET in Imaging Neurodegenerative Disorders,” *J. Nucl. Med.*, vol. 63, no. Supplement 1, pp. 13–19, 2022, doi: https://doi.org/10.2967/jnumed.121.263195.

[6] S. Garcia-Ptacek and M. G. Kramberger, “Parkinson Disease and Dementia,” *J. Geriatr. Psychiatry Neurol.*, vol. 29, no. 5, pp. 261–270, 2016, doi: 10.1177/0891988716654985.

[7] A. Lang and A. Lees, “Management of Parkinson’s disease: an evidence-based review,” *Mov. Disord.*, vol. 17, pp. 7–12, 2002, doi: https://doi.org/10.1002/mds.5555.

[8] A. Lees, “Alternatives to levodopa in the initial treatment of early Parkinson’s disease,” *Drugs and Aging*, vol. 22, no. 9, pp. 731–740, 2005, doi: 10.2165/00002512-200522090-00002.

[9] C. J. Langmead, J. Watson, and C. Reavill, “Muscarinic acetylcholine receptors as CNS drug targets,” *Pharmacology and Therapeutics*, vol. 117, no. 2. pp. 232–243, Feb. 2008. doi: 10.1016/j.pharmthera.2007.09.009.

[10] D. Dencker *et al.*, “Muscarinic acetylcholine receptor subtypes as potential drug targets for the treatment of schizophrenia, drug abuse, and Parkinson’s disease,” *ACS Chem. Neurosci.*, vol. 3, no. 2, pp. 80–89, 2012, doi: 10.1021/cn200110q.

[11] T. Haga, “Molecular properties of muscarinic acetylcholine receptors,” *Proc. Japan Acad. Ser. B Phys. Biol. Sci.*, vol. 89, no. 6, pp. 226–256, 2013, doi: 10.2183/pjab.89.226.

[12] S. Maeda, Q. Qu, and E. Al, “Structures of the M1 and M2 muscarinic acetylcholine receptor/G-protein complexes,” *Science (80-.).*, vol. 364, no. 6440, pp. 552–557, 2019, doi: 10.1126/science.aaw5188.

[13] M. Freissmuth, O. Stefan, and S. Böhm, *Pharmakologie und Toxikologie, 2. Auflage*. 2015.

[14] K. Aktories, U. Förstermann, F. Hofmann, and K. Starke, *Allgemeine und spezielle Pharmakologie und Toxikologie*, 10.Auflage. Elsevier, 2009.

[15] S. Verma, A. Kumar, T. Tripathi, and A. Kumar, “Muscarinic and nicotinic acetylcholine receptor agonists: current scenario in Alzheimer’s disease therapy,” *J. Pharm. Pharmacol.*, vol. 70, no. 8, pp. 985–993, 2018, doi: 10.1111/jphp.12919.

[16] R. M. Eglen, A. Choppin, and N. Watson, “Therapeutic opportunities from muscarinic receptor research,” *Trends Pharmacol. Sci.*, vol. 22, no. 8, p. 409, 2001, doi: https://doi.org/10.1016/S0165-6147(00)01737-5.

[17] A. Fisher, “Therapeutic strategies in Alzheimer’s disease: M1 muscarinic agonists,” *Japanese J. Pharmacol.*, vol. 84, no. 2. pp. 101–112, 2000. doi: 10.1254/jjp.84.101.

[18] M. Malviya, Y. C. Sunil Kumar, R. B. Mythri, C. Venkateshappa, M. N. Subhash, and K. S. Rangappa, “Muscarinic receptor 1 agonist activity of novel N-aryl carboxamide substituted 3-morpholino arecoline derivatives in Alzheimer’s presenile dementia models,” *Bioorganic Med. Chem.*, vol. 17, no. 15, pp. 5526–5534, 2009, doi: 10.1016/j.bmc.2009.06.032.

[19] S. Jiang *et al.*, “M1 muscarinic acetylcholine receptor in Alzheimer’s disease,” *Neurosci. Bull.*, vol. 30, no. 2, pp. 295–307, 2014, doi: 10.1007/s12264-013-1406-z.

[20] K. Haga *et al.*, “Structure of the human M2 muscarinic acetylcholine receptor bound to an antagonist,” *Nature*, vol. 482, no. 7386, pp. 547–551, 2012, doi: 10.1038/nature10753.

[21] J. Gomeza *et al.*, “Pronounced pharmacologic deficits in M2 muscarinic acetylcholine receptor knockout mice,” *Proc. Natl. Acad. Sci. U. S. A.*, vol. 96, no. 4, pp. 1692–1697, 1999, doi: 10.1073/pnas.96.4.1692.

[22] F. Shuaib, D. Kimbrough, M. Roofe, G. McGwin Jr, and P. Jolly, “Novel Insights Into M3 Muscarinic Acetylcholine Receptor Physiology and Structure,” *Bone*, vol. 23, no. 1, pp. 1–7, 2008, doi: 10.1007/s12031-013-0127-0.Novel.

[23] M. Ishii and Y. Kurachi, “Muscarinic Acetylcholine Receptors,” *Curr. Pharm. Des.*, vol. 12, no. 28, 2006.

[24] J. Jeon *et al.*, “A subpopulation of neuronal M4 muscarinic acetylcholine receptors plays a critical role in modulating dopamine-dependent behaviors,” *J. Neurosci.*, vol. 30, no. 6, pp. 2396–2405, 2010, doi: 10.1523/JNEUROSCI.3843-09.2010.

[25] D. J. Foster *et al.*, “M5 receptor activation produces opposing physiological outcomes in dopamine neurons depending on the receptor’s location,” *J. Neurosci.*, vol. 34, no. 9, pp. 3253–3262, 2014, doi: 10.1523/JNEUROSCI.4896-13.2014.

[26] E. Madorran, A. Stožer, S. Bevc, and U. Maver, “In vitro toxicity model: Upgrades to bridge the gap between preclinical and clinical research,” *Bosn. J. Basic Med. Sci.*, vol. 20, no. 2, pp. 157–168, 2020, doi: 10.17305/bjbms.2019.4378.

[27] O. Ciani and C. J.mmi, “The role of health technology assessment bodies in shaping drug development,” *Drug Des. Devel. Ther.*, vol. 8, pp. 2273–2281, 2014, doi: 10.2147/DDDT.S49935.

[28] M. Ozenil *et al.*, “Update on pet tracer development for muscarinic acetylcholine receptors,” *Pharmaceuticals*, vol. 14, no. 6, 2021, doi: 10.3390/ph14060530.

[29] J. Czernin, I. Sonni, A. Razmaria, and J. Calais, “The future of nuclear medicine as an independent specialty,” *J. Nucl. Med.*, vol. 60, no. 9, pp. 3S-12S, 2019, doi: 10.2967/jnumed.118.220558.

[30] L. Zhang and A. Villalobos, “Strategies to facilitate the discovery of novel CNS PET ligands,” *EJNMMI Radiopharm. Chem.*, vol. 1, no. 1, pp. 1–12, 2016, doi: 10.1186/s41181-016-0016-2.

[31] C. W. N. S. S. J. R. B. Usselman, “Positron Emission Tomography: Current Challenges and Opportunities for Technological Advances in Clinical and Preclinical Imaging Systems,” *Physiol. Behav.*, vol. 176, no. 3, pp. 139–148, 2017, doi: 10.1016/j.physbeh.2017.03.040.

[32] G. D. Rabinovici *et al.*, “11C-PIB PET imaging in Alzheimer disease and frontotemporal lobar degeneration,” *Neurology*, vol. 68, no. 15, pp. 1205 LP – 1212, Apr. 2007, doi: 10.1212/01.wnl.0000259035.98480.ed.

[33] G. G. H Brunner, M Veriá, P Polterauer, “Effect of pirenzepine, a new gastric acid-inhibiting agent, on exocrine pancreatic secretion in man,” *Arzneimittelforschung*, vol. 27, pp. 684–687, 1977.

[34] R. N. B. A A Carmine, “Pirenzepine. A review of its pharmacodynamic and pharmacokinetic properties and therapeutic efficacy in peptic ulcer disease and other allied diseases,” *Drugs*, vol. 30, pp. 85–126, 1985, doi: https://doi.org/10.2165/00003495-198530020-00001.

[35] M. Ozenil *et al.*, “Unexpected scaffold rearrangement product of pirenzepine found in commercial samples,” *Sci. Rep.*, vol. 11, no. 1, pp. 1–10, 2021, doi: 10.1038/s41598-021-02732-y.

[36] A. A. Gee, A.D.; Bongarzone, S.; Wilson, “Small Molecules as Radiopharmaceutical Vectors,” in *Radiopharmaceutical Chemistry*, B. M. Z. Jason S. Lewis, Albert D. Windhorst, Ed. 2019, pp. 119–136.

[37] C. Vraka, L. Nics, K. H. Wagner, M. Hacker, W. Wadsak, and M. Mitterhauser, “LogP, a yesterday’s value?,” *Nucl. Med. Biol.*, vol. 50, pp. 1–10, Jul. 2017, doi: 10.1016/j.nucmedbio.2017.03.003.

[38] C. A. Lipinski, F. Lombardo, B. W. Dominy, and P. J. Feeney, “Experimental and computational approaches to estimate solubility and permeability in drug discovery and development settings,” *Adv. Drug Deliv. Rev.*, vol. 64, no. SUPPL., pp. 4–17, 2012, doi: 10.1016/j.addr.2012.09.019.

[39] W. Abdullahi, D. Tripathi, and P. T. Ronaldson, “Blood-brain barrier dysfunction in ischemic stroke: Targeting tight junctions and transporters for vascular protection,” *Am. J. Physiol. - Cell Physiol.*, vol. 315, no. 3, pp. C343–C356, 2018, doi: 10.1152/ajpcell.00095.2018.

[40] V. W. Pike, “PET radiotracers: crossing the blood-brain barrier and surviving metabolism,” *Trends Pharmacol. Sci.*, vol. 30, no. 8, pp. 431–440, 2009, doi: 10.1016/j.tips.2009.05.005.

[41] T. . Riss, A. Niles, and L. Minor, *Cell Viability Assays*. Assay Guidance Manual [Internet], 2015.

[42] K. Abe and N. Matsuki, “Measurement of cellular 3-(4,5-dimethylthiazol-2-yl)-2,5-diphenyltetrazolium bromide (MTT) reduction activity and lactate dehydrogenase release using MTT,” *Neurosci. Res.*, vol. 38, no. 4, pp. 325–329, 2000, doi: 10.1016/S0168-0102(00)00188-7.

[43] E. CHACON, D. ACOSTA, and J. LEMASTERS, “Primary Cultures of Cardiac Myocytes as In Vitro Models for Pharmacological and Toxicological Assessments,” *Vitr. Methods Pharm. Res.*, pp. 209–223, 1996, doi: 10.1016/b978-012163390-5/50010-7.

[44] M. Qume, “Overview of ligand-receptor binding techniques.,” *Methods Mol. Biol.*, vol. 106, pp. 3–23, 1999, doi: 10.1385/0-89603-530-1:3.

[45] M. S. Salahudeen and P. S. Nishtala, “An overview of pharmacodynamic modelling, ligand-binding approach and its application in clinical practice,” *Saudi Pharm. J.*, vol. 25, no. 2, pp. 165–175, 2017, doi: 10.1016/j.jsps.2016.07.002.

[46] L. A. A. De Jong, D. R. A. Uges, J. P. Franke, and R. Bischoff, “Receptor-ligand binding assays: Technologies and applications,” *J. Chromatogr. B Anal. Technol. Biomed. Life Sci.*, vol. 829, no. 1–2, pp. 1–25, 2005, doi: 10.1016/j.jchromb.2005.10.002.

[47] H. Motulsky and R. Neubig, “Analyzing Radioligand Binding Data,” *Curr. Protoc. Neurosci.*, vol. 19: 7.5.1-, 2002, doi: https://doi.org/10.1002/0471142301.ns0705s19.

[48] C. A.Flanagan, “Chapter 10 - GPCR-radioligand binding assays,” *Methods Cell Biol.*, vol. 132, pp. 191–215, 2016.

[49] M. Ozenil *et al.*, “Synthesis, biological, and computational evaluation of antagonistic, chiral hydrobenzoin esters of arecaidine targeting machr m1,” *Pharmaceuticals*, vol. 13, no. 12, pp. 1–12, 2020, doi: 10.3390/ph13120437.

[50] https://www.protocols.io/view/counting-cells-with-hemocytometer-e6nvwyp7lmkj/v1 (accessed Jan. 22, 2023).

[51] https://www.emsdiasum.com/docs/technical/datasheet/68052-14 (accessed Jan. 22, 2023).

[52] https://expresslabwerks.com/products/brendel-m-48-cell-harvester (accessed Jan. 22, 2023).